Mineralogy and Petrology (1990) 42: 265–286

Mineralogy and Petrology

Platinum-Group Minerals in Quaternary Gold Placers in the Upper Chindwin Area of Northern Burma

D. Hagen[1], Th. Weiser[1], and Than Htay[2]

[1] Federal Institute for Geosciences and Natural Resources, Hannover, Federal Republic of Germany, [2] Department of Geological Survey and Exploration, Rangoon, Burma

With 8 Figures

Received August 3, 1989;
accepted December 6, 1989

Abstract

In the Chindwin Basin in northern Burma, there is a system of five Pleistocene terraces in which gold placers with low concentrations of platinum-group minerals (PGM) occur. Samples were taken from four sites in the Chindwin Basin and one from near an ophiolite occurrence on the northeast side of the Chindwin Basin; they were studied under the microscope, with a scanning electron microscope, and an electron microprobe. The main minerals were Pt-Fe and Os-Ir-Ru alloys, usually in a ratio between 2 and 5. In most cases, the shape of the grains allowed a quick distinction between the two types. Sperrylite, laurite, irarsite, cooperite, tulameenite, and isomertieite occur infrequently as individual mineral grains and sometimes as inclusions in the alloy grains. Braggite, platarsite, hollingworthite, bowieite, keithconnite, cuproiridsite, malanite, stibiopalladinite, geversite, kashinite, several unnamed PGM, and Fe, Ni, and Cu sulfides were observed as inclusions, mainly in the Pt-Fe alloys and also to a lesser extent in the Os-Ir-Ru alloys. Lamellar and myrmekite-like intergrowths, oriented exsolution lamellae, and idiomorphic inclusions of sulfides in the alloys indicate a magmatic origin of the PGM. The origin of the PGM is assumed to be ophiolites in northern Burma. A continual decrease in mean grain size occurred during transport.

Zusammenfassung

Platingruppenminerale in quartären Goldseifen im oberen Chindwingebiet in Nord-Burma

Im Gebiet des Chindwin Basin in Nordburma ist ein System von fünf pleistozänen Terrassen ausgebildet, in denen Goldseifen mit geringen Anteilen an PGM auftreten.

PGM-Konzentrate von vier Vorkommen des Chindwin Basin und eine weitere Probe aus der Nähe eines Ophiolithvorkommens im Nordosten des Chindwin Basin

wurden mit optischer Mikroskopie, Rasterelektronenmikroskopie und Mikrosonde untersucht.

Hauptmineralien sind Pt-Fe-Legierungen und Os-Ir-Ru-Legierungen in einem Verhältnis von 2 : 1 bis 5 : 1. Ihre Morphologie kugeliger oder plattiger, teilweise idiomorpher Körner erlaubt in den meisten Fällen eine rasche Identifizierung der beiden Typen. Sehr selten treten als Einzelminerale, aber auch als Einschlüsse in Legierungen, Sperrylith, Laurit, Irarsit, Cooperit, Tulameenit und Isomertieit auf. Braggit, Platarsit, Hollingworthit, Bowieit, Keithconnit, Cuproiridsit, Malanit, Stibiopalladinit, Geversit, Kaschinit, einige unbekannte PGM und Fe-, Ni- und Cu-Sulfide wurden nr als Einschlüsse, hauptsächlich in Pt-Fe-Legierungen, weniger in Os-Ir-Ru-Legierungen, beobachtet.

Lamellare und myrmekitische Verwachsungen, orientierte Entmischungen und idiomorphe Einschlüsse von Sulfiden in Legierungen weisen auf eine magmatische Entstehung der PGM hin. Die Herkunft der PGM wird in Ophiolithen Nordburmas vermutet. Beim Transport hat eine kontinuierliche Abnahme der mittleren Korngrösse stattgefunden.

Introduction

The Federal Institute for Geosciences and Natural Resources (BGR) has been conducting a project, "Eastern Chin Hills and Arakan Yoma Mineral Survey" (ECAMS), within the framework of Technical Cooperation with Burma since 1980. The objective is the systematic exploration of the Indoburman ranges and adjacent areas in Burma. Within the scope of this project, unconsolidated Quaternary sediments along the lower Uyu and the upper Chindwin rivers have been explored for gold and platinum-group minerals (PGM) since 1982. The study area is around Homalin, about 1000 km north of Rangoon (Fig. 1). Studies on the stratigraphy, genesis, and regional distribution of the Quaternary terraces were begun in 1987. These were concluded in 1988 with the participation of *H. J. Unger* from the Bavarian Geological Survey.

Although the PGM in the study area are not of particular economic interest, they are of considerable scientific interest because no primary PGM occurrences are known in Burma that could be the source rocks. Secondary PGM occurrences in alluvial deposits in northern Burma are mentioned in the literature (e.g. *Goossens*, 1978), but they had not been scientifically studied. In this paper, we will give the first description of PGM in Pleistocene placers on the Uyu and Chindwin Rivers and in the area around Lake Indawgyi.

Geological Evolution of the Area

During the collision of the Indian Plate with the Asian Plate, an outer island arc was formed offshore to the east beginning in the Upper Eocene (*Bannert* and *Helmcke*, 1981). This led to the emplacement of an ophiolite suite. The ultrabasic part of this suite consists of serpentinized to carbonatized harzburgites, lherzolites, dunites, and pyroxenites (*Bender*, 1983; *Chattopadhyay* et al., 1983). Gabbros and basalts are also present. Chromium and nickel mineralizations are associated with the ultrabasic rocks. Pyrite and chalcopyrite deposits occur in the basaltic rocks. Concurrently with the formation of the outer island arc, the Western Burma Plate drifted northwards, resulting in a complicated distribution of these ophiolites in

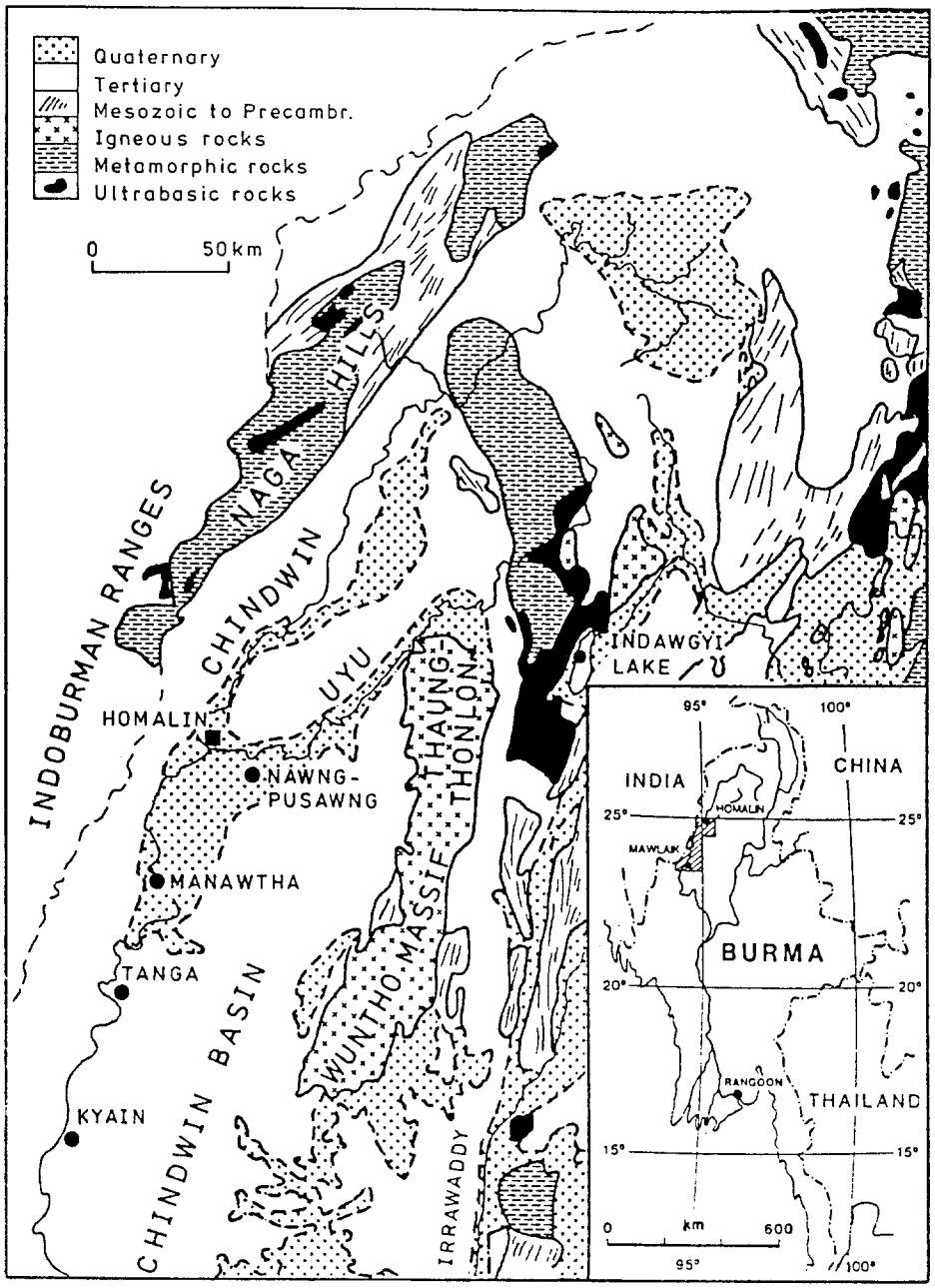

Fig. 1. Location map showing geology (after *Bender*, 1983). Quaternary modified by *Hagen*

northern Burma. Finally in the late Tertiary, the Indoburman ranges were formed from this island arc and forced against the Himalayas. Beginning in the Miocene, the Chindwin Basin was formed between the Indoburman ranges in the west and the continental block of the Sinoburman ranges in the east. Volcanic rocks occur near Monywa and on Mt. Popa along the axis of the Chindwin Basin, as well as in the Wuntho Massif, and in the area around Mt. Thaungthorlon. These rocks, together with calc-alkaline plutonites, form the inner island arc. Volcanic activity continued until the late Pleistocene. Copper and gold deposits in these volcanic rocks are known near Monywa and in the Wuntho Massif.

Since the beginning of the Pleistocene, uplifting of the Chindwin Basin has resulted in an extensive system of Pleistocene terraces along the Chindwin and Uyu rivers. Gold placers containing a small proportion of PGM have been found in these terraces; various types of primary gold mineralizations and ophiolitic rocks at the margins of the basin are assumed to be the source for these placers.

Sediment Petrography

Five petrographically similar Pleistocene terraces (T_0 to T_4, Fig. 2) occur in the Chindwin-Uyu area. The sequence begins in each case with a layer of poorly sorted gravel containing clastic components of clayey silt to cobbles. These gravel beds are up to 15 m thick and rapidly wedge out laterally or grade into fine gravel to sand. They are covered with clayey to fine-sandy silt up to 10 m thick; laterization has advanced deeply into this layer, coloring it red-brown. The pebbles are well rounded. The petrographic composition does not vary within any one of the terraces or from one terrace to the next. This indicates extensive reworking. The main components are quartz and quartzite; colored chert occurs in varying amounts, usually between 5 and 10%. Crystalline pebbles are rare. Ultrabasic rocks were seldom observed; they were found in the <6.3-mm fraction, usually silicified. Soft Tertiary rocks are rare but locally may make up as much as 40% of the gravel.

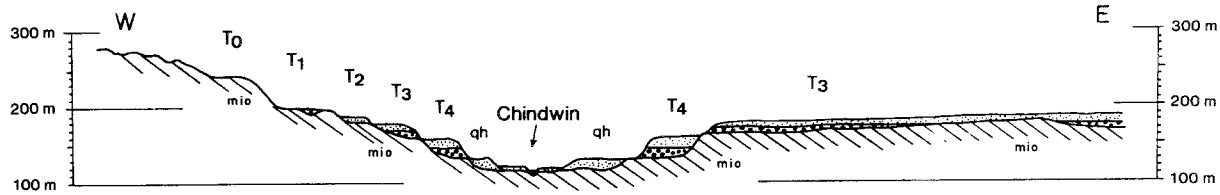

Fig. 2. Pleistocene terraces around Myenga, 30 km S of Homalin; elevations in meters above m.s.l.; *mio* = Miocene/Tertiary; vertical exaggeration 2 : 1

The heavy mineral fraction consists mainly of opaque minerals, usually hematite and ilmenite, sometimes with traces of magnetite and chromite. The gold contents are usually very low; only in very small areas are economic concentrations present. The PGM concentrations are seldom more than 5 wt.% of the gold values. In the southern part of the study area, however, the PGM/gold ratio approaches unity. Maximum grain size, composition of the gravel, and the heavy mineral assemblage in the Pleistocene gravel differ considerably from those of the Tertiary. The Tertiary sediments of the northern Chindwin Basin are considerably more fine-grained (*Reimann* and *Aye Thaung*, 1981) than those of the Pleistocene terraces. North of the study area, the Tertiary sediments along the Chindwin River are fine sand to silt; in the Uyu Anticline between the Chindwin and Uyu Rivers NE of Homalin, the coarsest Tertiary rocks are coarse sandstones containing a small amount of fine gravel. For this reason it is concluded that the very coarse Pleistocene gravels and their metal content are not derived in the main from reworked Tertiary but were transported by the early Chindwin and Uyu rivers from the northern margin of the Chindwin Basin. Tertiary components in the Pleistocene terraces are mainly the fine-sandy, silty matrix of the gravel and the fine-clastic cover layer.

Five representative concentrate samples were selected to determine the grain-size distribution. Four samples were taken in the study area at uniform distances from each other over a distance of 200 km. From north to south, the samples were taken from a Pleistocene gold field near Nawngpusawng (T_3 terrace) on the Uyu River, the Manawtha gold field (T_4), the Tanga gold field (T_3 or T_4), and the gold fields around Kyain (T_4), the last three sites being along the Chindwin River (Fig. 1). A sample was also taken from alluvium on the west bank of Lake Indawgyi near a large ultrabasic rock body of unknown petrographic composition. This site is about 100 km northeast of Nawngpusawng, outside the study area.

Laboratory sample no.	Sampling site	Weight (g)	Number of PGM grains
#2272	Nawngpusawng	8.4399	ca. 190 000
#3088	Manawtha	0.0104	234
#3089	Tanga	3.4200	ca. 350 000
#3374	Kyain	0.5499	ca. 51 000
#3452	Lake Indawgyi	0.5736	920

Seven fractions between <63 μm and 2000 μm were sieved. The largest grain was a Pt-Fe platelet with a maximum diameter of 4200 μm (from Lake Indawgyi). The smallest grain measured 45 μm across (Fig. 3h).

The most important result was the difference in median grain diameter between the Lake Indawgyi sample, which was taken close to a possible source area, and the samples from the Chindwin Basin. In the Chindwin Basin, the median diameter from the cumulative curves decreased from 140 μm at Nawngpusawng and Manawtha to 85 μm downstream at Tanga and Kyain. The comparison sample taken at Lake Indawgyi had a median diameter of 270 μm. Further, the mean weight per grain in the 355–630-μm fraction decreased from 1.3 mg at Lake Indawgyi to 0.4 mg at Kyain, in the 200–355-μm fraction it decreased from 0.24 mg to 0.07 mg, and in the 112–200-μm fraction it decreased from 0.06 to 0.02 mg. These numbers show decreasing thickness of the grains during transport. In contrast, no decrease was found in the mean weight of the grains in the 63–112-μm and <63-μm fractions. This is explained by the near absence of platy grains and the predominance of spherical grains in these fractions.

Analytical Methods

Some of the grains were mounted on an aluminum target and coated with a thin layer each of carbon and gold so that they could be examined with a scanning electron microscope equipped with an energy dispersive analysis system.

For optical and microprobe examination, parts of the samples were mounted in epoxy resin and polished with diamond powder.

The microprobe analyses were done with a Camebax Microbeam from Cameca Instruments. An accelerating voltage of 20 kV was used with a 15 nA beam current and 10 s measurement time. The x-ray intensities were corrected using the PAP computer program of Cameca Instruments. Fifteen elements were determined using the following standards and spectral lines:

standard	line	standard	line
ruthenium metal	Ru Lα	rhodium metal	Rh Lα
osmium metal	Os Mα	iridium metal	Ir Lα
gold metal	Au Lα	silver metal	Ag Lβ
copper metal	Cu Kα	nickel metal	Ni Kα
pyrite	S Kα	synthetic Pt_3Fe alloy	Pt Lα and Fe Kα
synthetic Pd_3HgTe_3	Te Lα	synthetic GaAs	As Lα
stibnite	Sb Lα	bismuthinite	Bi Mα
synthetic PdS	Pd Lα	galena	Pb Lβ

The enhancement of the primary x-ray lines by secondary lines of other elements was corrected for mathematically:

primary line	secondary line(s)
Rh Lα	Ru $L\beta_1$ and Pt M II
Pd Lβ	Ag Lα
Ag Lβ	Rh $L\gamma_1$ and Pt Lα
Cu Kα	Ir L_1
As Lα	Ru LαII and Sb $L\beta_1$
Sb Lα	Te L_n

A total of 546 quantitiative analyses were made on grains and inclusions from the samples from the five sampling sites.

Stereo Microscopy and Scanning Electron Microscopy

The five PGM samples consist almost entirely of two groups of minerals: Pt-Fe alloys and Os-Ir-Ru alloys, usually in a ratio between 2 and 5. As seen under the stereomicroscope, the Pt-Fe alloy grains are mostly thick, rounded plates with diameters of up to 4 mm. The surfaces are rough (Fig. 3: e and h), often showing scratches from transport; they have a dull metallic luster, often with a brown to bronze hue. Iron oxide coatings were frequently observed, especially in the grain-size fractions 112–355 μm. The grains were seldom irregular, lobed, or elongated (Fig. 3: l, n, and o). Pt-Fe alloys are present in the fractions < 112 μm in the form of cubic crystals (see below).

Fig. 3. SEM photomicrographs of PGM grains from the Chindwin-Uyu area, northern Burma. a) Os-Ir-Ru alloy; Nawngpusawng gold field on the Uyu River. b) Os-Ir-Ru alloy; Hwephugon gold field, 6 km NW of Manawtha on the Chindwin River. c) Os-Ir-Ru alloy; Kyain gold field on the Chindwin River. d) Os-Ir-Ru alloy; Kyain gold field. e) Os-Ir-Ru alloy; Kyain gold field. f) Os-Ir-Ru alloy; Kyain gold field. g) sperrylite (left) and Pt-Fe alloy (right); Yohla gold field, 20 km N of Kyain. h) Pt-Fe alloy; Yohla gold field, 20 km N of Kyain. i) Os-Ir-Ru alloy; Hwephugon gold field, 6 km NW of Manawtha. k) Pt-Fe alloy (light) grown together with Os-Ir-Ru alloy (dark); Nansima gold field, 25 km S of Manawtha. l) Pt-Fe alloy; Yohla gold field, 20 km N of Kyain. m) Os-Ir-Ru alloy; Tatkon gold field, 25 ▶

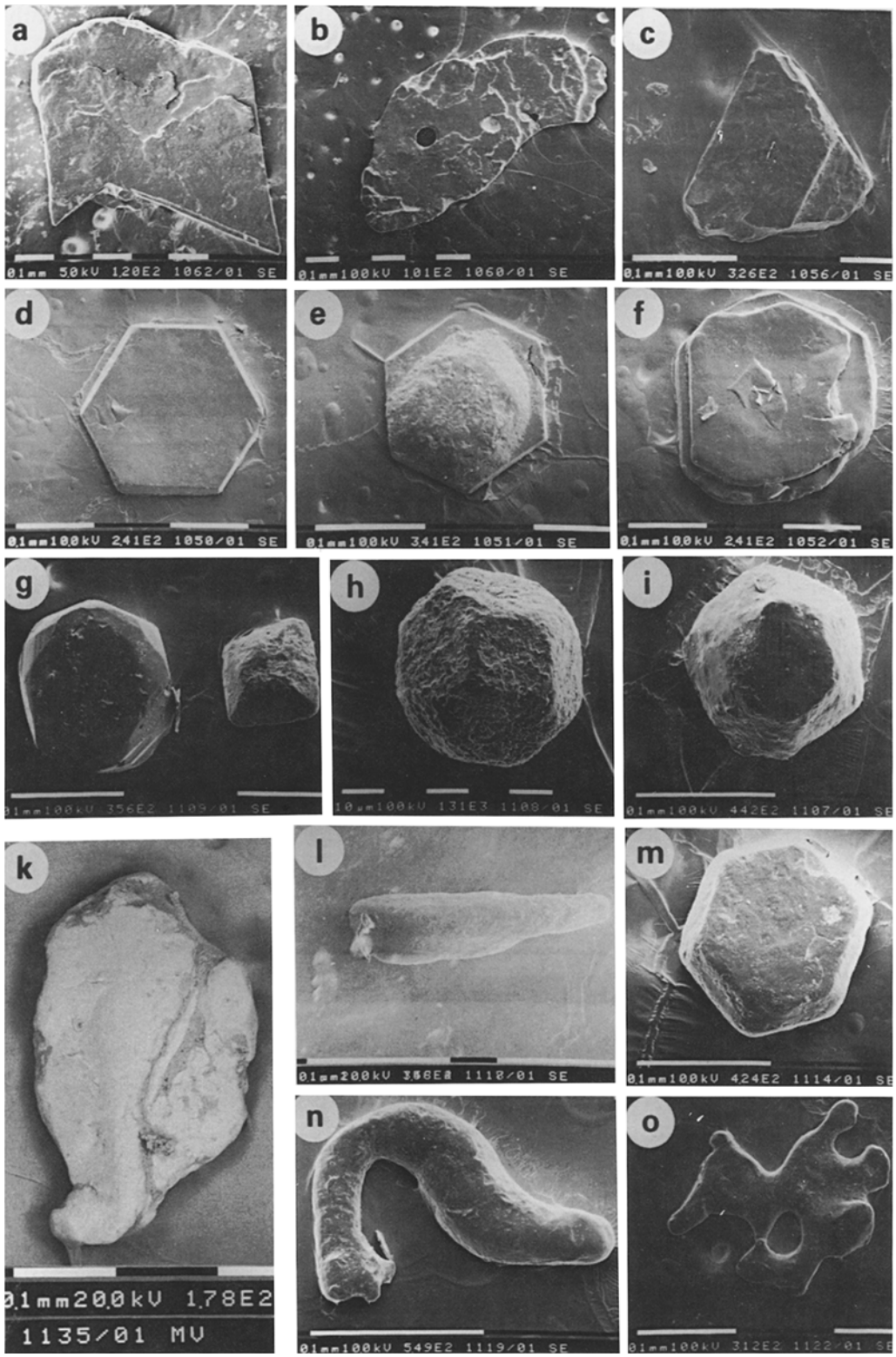

Fig. 3. (continued)
km SSW Tanga. n) Pt-Fe alloy; Manawtha gold field on the Chindwin River. o) Pt-Fe alloy; Simaw gold field, 30 km S of Manawtha

In contrast to the Pt-Fe alloys, the Os-Ir-Ru alloy grains have very smooth surfaces with metallic luster. The fracture surfaces often show 120° angles (Fig. 3a). Perfect hexagonal thin platelets are rare in the grain-size fractions <200 μm (Fig. 3: d, e, and f). Some grains have the form of an equilateral triangle (Fig. 3c). Very often, cleavage planes can be recognized; sometimes depressions or holes with a hexagonal outline occur (Fig. 3b). In a number of cases, sausage- or cup-shaped Pt-Fe alloy was found grown on a hexagonal Os-Ir-Ru platelet; in polished section, such grains were seen to have a straight-line contact between the two alloys. An example of two Os-Ir-Ru platelets grown together is shown in Fig. 3f. A composite grain of Pt-Fe alloy (light colored) and Os-Ir-Ru alloy (dark colored) is shown in Fig. 3k.

In the <112-μm grain-size fractions, mainly spherical PGM grains were observed. In the scanning electron microscope these were seen to be cubic or hexagonal crystals more or less rounded at the corners. An octahedral Pt-Fe alloy is shown on the right in Fig. 3g, a combination of a cube and an octahedron is shown in Fig. 3h. The energy dispersive analysis of the crystal at the left in Fig. 3g shows spectral lines for Pt and As, indicating that the grain is probably sperrylite. The crystals in Figs. 3i and 3m consist of Os-Ir-Ru alloys.

Mineralogy

The main minerals in all of the samples are Pt-Fe and Os-Ir-Ru alloys. They make up about 96% of the samples. The other PGM that occur as discrete grains in the samples are sperrylite, laurite, irarsite, cooperite, tulameenite, and isomertieite (in decreasing order of abundance). These minerals also occur as inclusions in the alloys. All other PGM described below occur only as inclusions in the alloys or form a composite grain with them.

Pt-Fe Alloys

The Pt-Fe alloy grains examined vary between 50 μm and 3 mm in diameter. The grains were usually rounded or had a lobed outline. Their color under the ore

Table 1. *Microprobe analyses of Pt-Fe alloys*

Analysis	Ru	Rh	Pd	Os	Ir	Pt	Fe	Cu	Ni	Total
2272a/ 10		1.16	0.59	1.13	14.33	78.74	5.13	0.42		101.50
/ 24		0.82		1.01	0.64	92.76	4.37	0.28		99.88
/112	0.27	1.43	8.38	1.15	3.86	77.14	4.19	0.65		97.06
2272b/ 65				0.38	0.25	77.14	16.37	3.09	2.26	99.49
3088 / 66	0.30	0.99		0.75	2.39	89.92	4.09	0.29		98.72
/128		1.04	8.79	0.47	4.90	73.94	7.55	0.41		97.09
3089a/ 30			11.53	0.35	2.68	73.22	9.77	0.85	0.50	98.90
/ 31			28.51	0.27	1.30	55.78	10.71	1.53	0.50	98.60
/ 49		1.34	0.94	1.00	1.35	89.63	5.15	0.38		99.79
/ 54		1.09	11.25	0.92	3.14	79.86	1.23	2.21		99.70
3374 / 44		0.74	0.65	0.40	1.82	82.85	12.56	0.56		99.57
3452 / 41		0.52		0.22	4.61	72.66	14.61	0.51	6.53	99.66

microscope was usually white but next to the Os-Ir-Ru alloys they had a distinct cream color. The size and number of inclusions varies greatly. The most common inclusions were drop- or lathe-shaped iridosmine and osmium crystals or idiomorphic laurite crystals. In most cases the osmium lamellae are too small for an exact

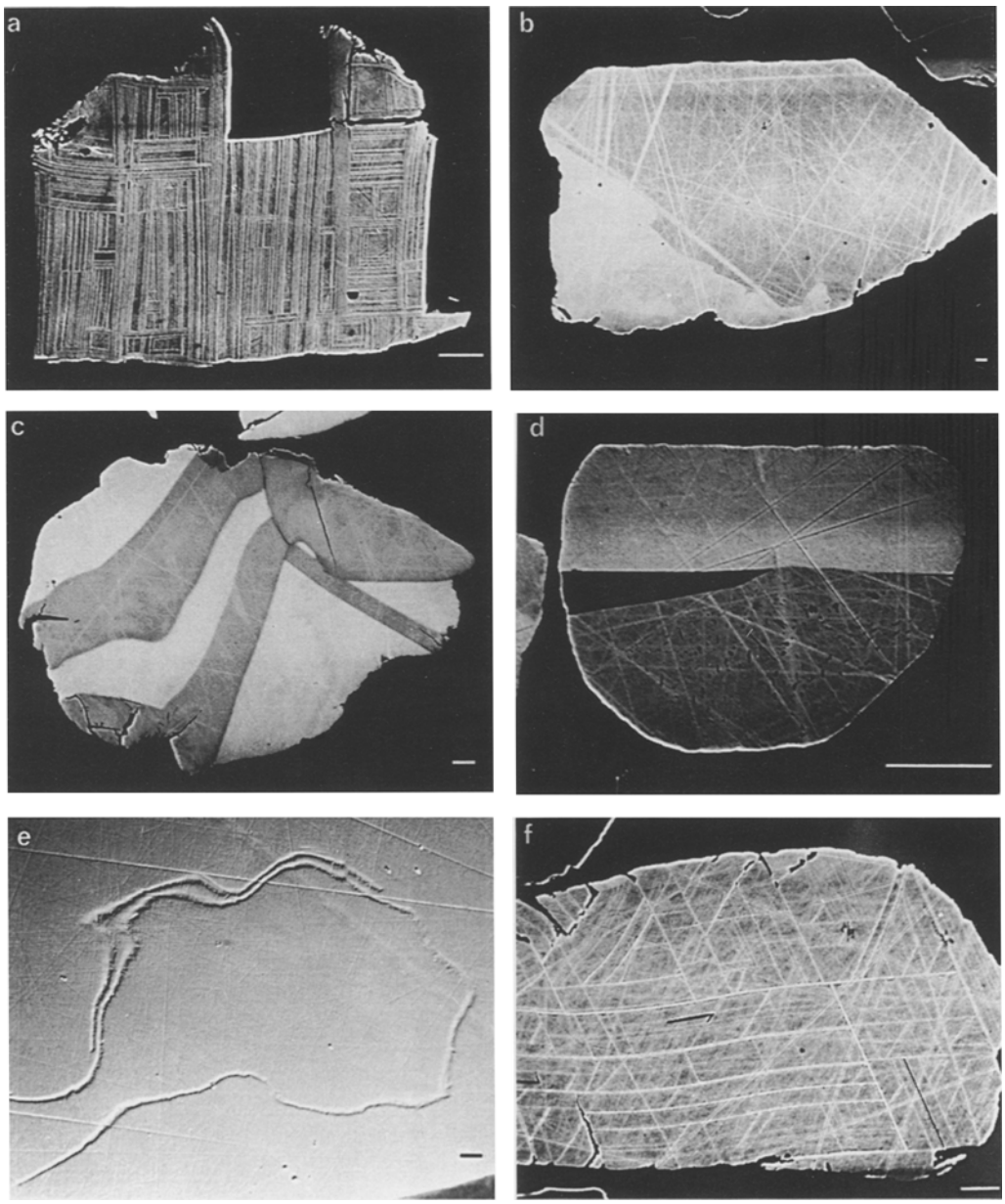

Fig. 4. Backscattered electron images (BEI) of Pt-Fe and Os-Ir-Ru alloys. a) Lamellar intergrowth of Pt-Fe alloy (dark) and Rutheniridosmine (light); Tanga. b) Iridosmine (light) in contact with osmiridium (dark); Nawngpusawng. c) Lamellar intergrowth of Pt-Fe alloy (dark) and rutheniridosmine (light); Manawtha. d) Rutheniridosmine (upper part) in contact with ruthenosmiridium (lower part) and a wedge of Pt-Fe alloy (black) in between; Manawtha. e) Schlieren-like exsolution of Pt-Fe alloy in rutheniridosmine; Lake Indawgyi. f) Pt-bearing osmiridium (dark) with oriented lamellae of rutheniridosmine (light); Nawngpusawng. Scale bar represents 10 μm

quantitative analysis and can only be detected qualitatively. The inclusions in the Pt-Fe alloy grains include almost all of the minerals described in this paper. The composite grains with the Os-Ir-Ru alloys frequently had sharp grain boundaries. Occasionally, lamellar intergrowths of these two minerals were found (Fig. 4: a and c). Pt-Fe alloys also occurred as oriented lamellae (either straight or wavey) in Os-Ir-Ru alloys (Fig. 4e). Replacement (by cooperite or irarsite) at the margins is rare.

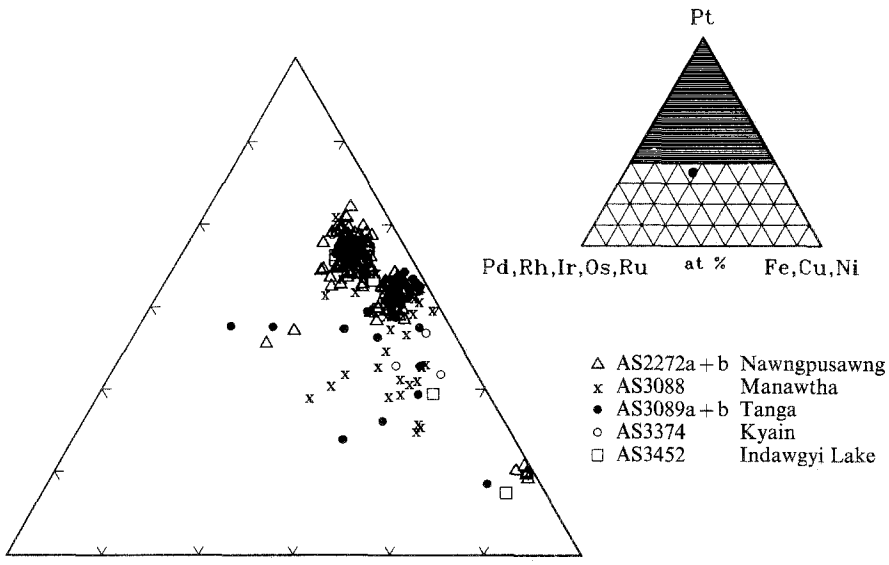

Fig. 5. Microprobe analyses of natural Pt-Fe alloys

Microprobe analysis showed that most of the Pt-Fe alloys have a composition near isoferroplatinum (Pt_3Fe), in only a few cases was the atomic ratio near unity (Fig. 5). Because a structure determination was not possible, we apply the nomenclature of *Cabri* and *Feather* (1975) and use the general name "Pt-Fe alloy". It is worthy of note, however, that inclusions of antimony minerals (e.g. geversite and stibiopalladinite) and the unnamed phases $(Pt, Pd)_2PbSb$ and Pd_2CuSb were observed only in the Pt-Fe alloys with a Pt/Fe atomic ratio of 1. With few exceptions, the Pt concentration of the Pt-Fe alloy grains was between 60 and 82 at.%, mostly between 70 and 80 at.%. The Fe + Cu + Ni content ranged between 13 and 29 at.%. Although the content of the other PGE in most of the grains was only 0–10 at.%, these elements showed the greatest variations. High Pd concentrations (#3089a/31) of up to 28 wt.% and high Ir concentrations (#2272a/10) of up to 14 wt.% were observed in grains and in inclusions of Pt-Fe alloys in the samples from Tanga and Nawngpusawng. All of the other PGM and Ni and Cu were observed only in traces. Gold and silver were not detected.

Os-Ir-Ru Alloys

The individual crystals, similar to those of the Pt-Fe alloys, are between 50 μm and 3 mm across. In polished section, they appeared mostly as white platelets with a

light blue tinge. In a few cases, composite grains of different phases of the Os-Ir-Ru system were identified under the microscope on the basis of slight differences in color (Fig. 4: b and d). The anisotropy of the hexagonal phases vary from weak to very strong depending on the orientation of the grain; the interference color varies from orange to dark brown. Undulating extinction was often observed and a distinct cleavage was frequently seen. Cubic phases seldom occurred.

Microprobe analyses showed the presence of all phases (nomenclature of *Harris* and *Cabri*, 1973) of the Os-Ir-Ru system except iridium and ruthenian iridium. Most of the grains in all of the samples had a composition of rutheniridosmine with varying Ru contents (Fig. 6). This corresponds to the data of *Harris* and *Cabri* (1973) for Papua New Guinea and *Tarkian* (1987) for the Ural Mts. The placer deposits in Tasmania contain also mainly rutheniridosmine, but with a much lower ruthenium content (*Ford*, 1981). This may indicate differences in the chemical composition of the ophiolitic source rocks.

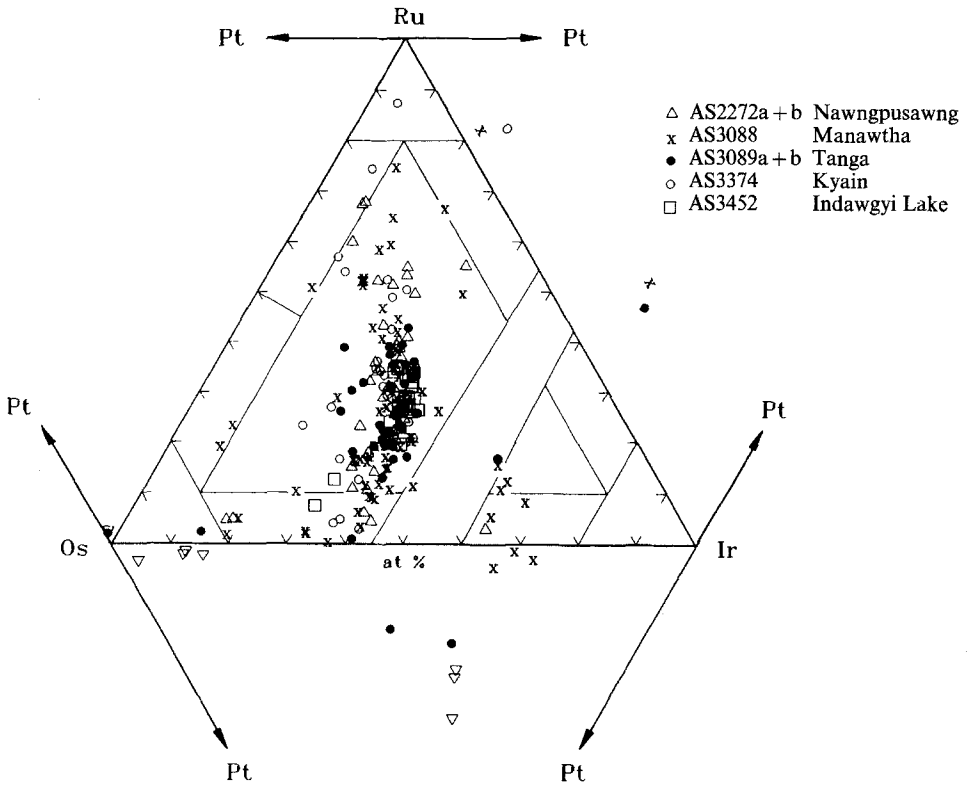

Fig. 6. Microprobe analyses of natural Os-Ir-Ru, Os-Ir-Pt, Ru-Ir-Pt, and Ru-Os-Pt alloys

All of the other phases of the system occur in only minor amounts. One each of the following cases was observed in which hexagonal and cubic phases were grown together: rutheniridosmine with ruthenosmiridium (Fig. 4d), ruthenosmiridium with osmiridium, and iridosmine with osmiridium (Fig. 4b). This was also observed by *Cabri* and *Harris* (1975) in Tasmania. Our studies also confirm the miscibility gap proposed by *Harris* and *Cabri* (1973), although some of the results seem to make a modification of their boundaries necessary (#3088/78 + 102, #3089b/5) (Fig. 6).

In some of the grains and exsolution lamellae very high Pt concentrations occur in the Os-Ir-Ru system (up to 34 at.%) (#2272a/68) and the Ru-Ir-Pt system (up to 17 at.%) (#3088/40), but not in the Ru-Os-Pt system. These grains occasionally contain very fine, oriented exsolution lamellae of Os-Ir-Ru alloys (Fig. 4f). Pt-Fe

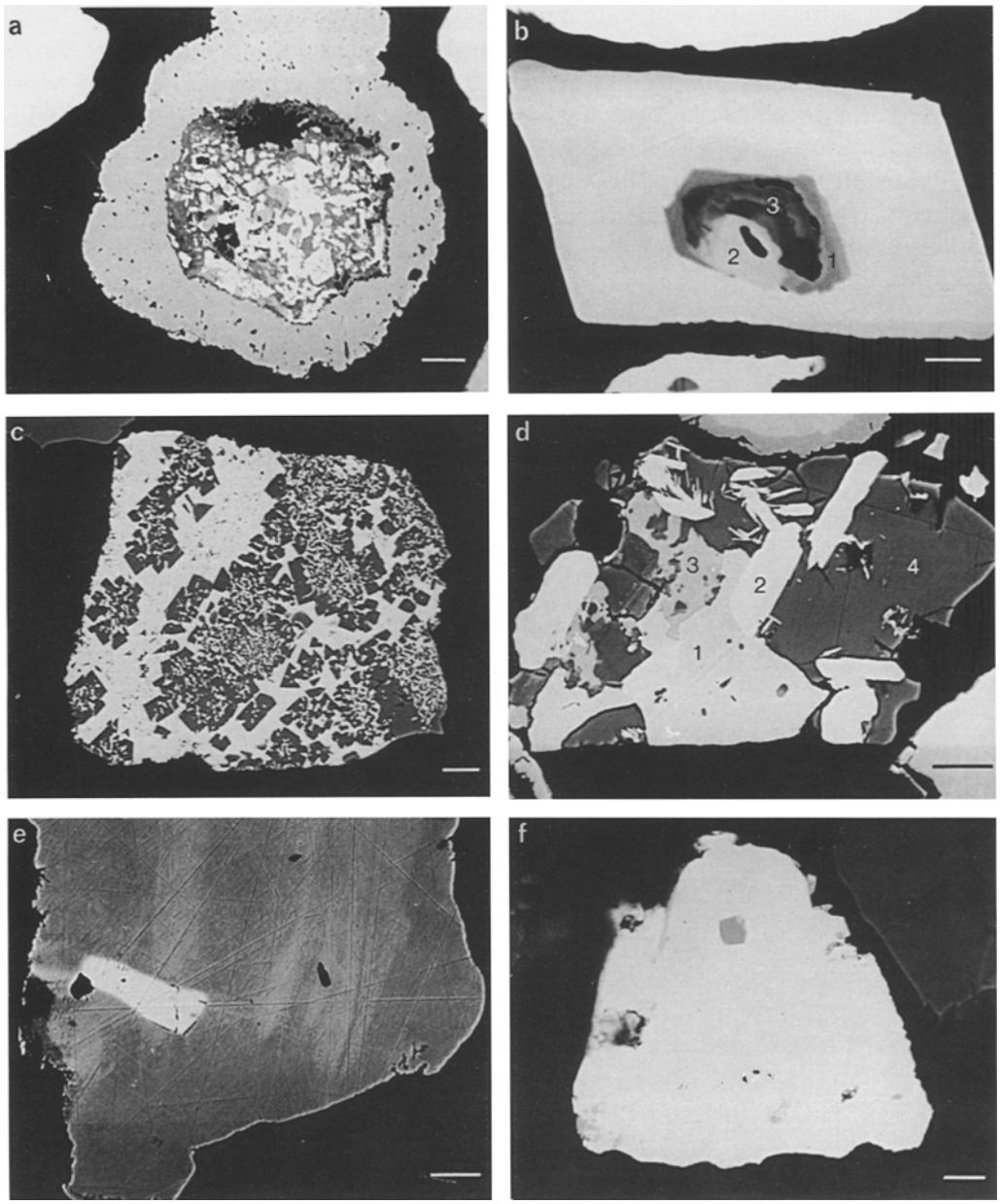

Fig. 7. Backscattered electron images (BEI) of various PGM. a) Intergrowth of native gold, sperrylite, hollingworthite and platarsite surrounded by sperrylite; Manawtha. b) Euhedral crystal of sperrylite with an inclusion consisting of (*1*) hollingworthite, (*2*) irarsite, and (*3*) laurite; Manawtha. c) Myrmekite-like intergrowth of Os-Ir-Ru (light) and laurite (dark); Nawngpusawng. d) Breccia-like intergrowth of (*1*) Pt-Fe alloy, (*2*) iridosmine, (*3*) cooperite, and (*4*) cuproiridsite; Manawtha. e) Pt-Fe alloy with inclusion of an unnamed PGM phase, probably $(Pt, Pd)_2PbSb$; Nawngpusawng. f) Pt-Fe alloy with inclusion of an unnamed PGM phase, probably $Rh_2Ni_3S_6$; Tanga. Scale bar represents 10 μm

alloys also occur in Os-Ir-Ru alloys (Fig. 4e). Other inclusions are rare, the most common of which is oriented pentlandite. The Os-Ir-Ru alloy is occasionally replaced by laurite or irarsite at the margins.

Table 2. *Microprobe analyses of Os-Ir-Ru-Pt alloys*

Analysis	Ru	Rh	Pd	Os	Ir	Pt	Fe	Cu	Ni	Total
2272a/ 68	5.57	1.66		21.74	37.05	30.58	2.97	0.38	0.27	100.21
/122	19.89	1.54		41.21	31.65	5.34				99.63
2272b/ 5	0.75			81.57	14.44	1.63				98.39
3088 / 14	1.04	0.60		25.98	70.60	3.06	0.31			101.59
/ 17	3.09	0.65		32.39	63.12	2.11	0.26			101.61
/ 31	34.97	0.31		51.79	11.06					98.13
/ 40	19.26	2.29		4.16	51.80	18.88	0.89	2.73		100.00
/ 56	47.32	0.69		12.90	31.76	6.70	0.71		0.19	100.26
/ 67	5.51	1.01		26.19	57.78	8.85	1.40		0.28	101.02
/ 78	8.03	2.55		24.69	55.60	8.90	0.63			100.40
/ 84	13.15	0.64		70.22	9.34	4.47				97.81
/102	6.46			44.59	48.51		0.79			100.34
3089a/ 43	1.23	0.36	0.20	81.81	13.93	2.28				99.81
/ 55	1.61	1.67		30.64	46.91	18.71	1.10			100.64
/ 74	0.21	0.55		95.62	0.27	1.16				97.81
3089b/ 5	8.81	2.85		24.99	56.74	7.04	0.76		0.22	101.41
3374 / 18	76.83	0.77	0.19	12.88	8.27					98.94
/ 35	53.59	5.28	0.25	4.59	24.50	10.63	0.47			99.30
3452 / 42	4.03			62.17	31.63		0.40			98.22

Sperrylite

Although it is the third most common mineral, it was observed only in the sample from Manawtha. The crystals were 125 μm across and usually idiomorphic. The analyses showed that the crystals were very pure and stoichiometric (#3088/86).

Table 3. *Microprobe analyses of sperrylite* $PtAs_2$

Analysis	Ru	Rh	Pd	Os	Ir	Pt	S	Te	As	Total
3088 / 4		0.23		0.21	14.59	38.36		7.64	36.71	97.73
/ 86				0.20		55.24			43.81	99.25
/120				0.23	0.26	55.83			43.59	99.91
/127	0.97	2.26		0.75	0.36	52.00	1.72		40.96	99.03

One grain of sperrylite, about 100 μm across, was unusual owing to its core, which consisted of a fine-grained intergrowth of gold, sperrylite, platarsite, and hollingworthite (Fig. 7a). We interpreted this structure as a primary intergrowth of these minerals with a later growth of sperrylite.

An oval inclusion was observed in one euhedral sperrylite crystal 120 μm long. This inclusion consists of intergrown laurite, hollingworthite, and irarsite (Fig. 7b).

Sperrylite intergrown with isomertieite also occurred as an inclusion about 20 μm across in Pt-Fe alloys. In this case it contained 14 wt.% Ir and 7 wt.% Te substituting As (#3088/4).

Laurite

As individual crystals, laurite was observed in only one sample from Nawngpusawng. These euhedral crystals were up to 150 μm across and abraded at the edges. Occasionally myrmekite-like intergrowth with Os-Ir-Ru alloys was observed (Fig. 7c). Laurite occurred mainly as euhedral crystals up to 20 μm across grown together with bowieite or hollingworthite as inclusions in Pt-Fe or Os-Ir-Ru alloys. The microprobe analyses showed that laurite often contained no Os and little Ir (Fig. 8). In the sample from Manawtha, an unusual high Rh content of 18 wt.% was determined in laurite (#3088/141).

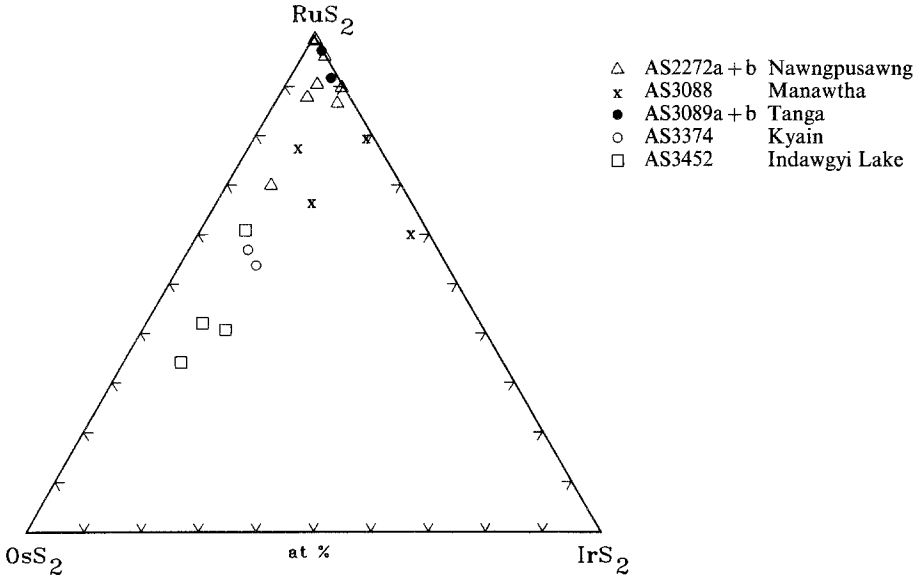

Fig. 8. Microprobe analyses in the RuS_2-OsS_2-IrS_2 system

Erlichmanite

Erlichmanite was observed only in the sample from Lake Indawgyi, where it replaces rutheniridosmine (#3452/25).

Table 4. *Microprobe analyses of laurite RuS_2/erlichmanite OsS_2*

Analysis	Ru	Rh	Pd	Os	Ir	Pt	Fe	Ni	S	As	Total
2272b/ 13	49.22	1.36		7.70	1.65	1.08			36.51		97.51
/ 18	58.63	0.21			0.22				38.01		97.07
3088 / 90	46.76	10.30		1.26	0.81	1.44			37.59		98.15
/141	34.82	18.91		3.26	2.25	2.41	2.42	0.59	35.99		100.65
3374 / 8	28.35			30.89	9.57				30.22	1.75	100.78
3452 / 25	14.78			45.58	8.18				28.13		96.67

Irarsite

This mineral occurred only seldom; fragments up to 250 μm across were observed in the samples from Nawngpusawng and Manawtha. They were very pure and stoichiometric (#2272a/158). More often, it occurs as replacement mineral on the margins of Pt-Fe and Os-Ir-Ru alloys. The concentrations of other PGM determined in these cases are most probably derived from the replaced mineral (#3089a/34).

Table 5. *Microprobe analyses of irarsite IrAsS*

Analysis	Ru	Rh	Pd	Os	Ir	Pt	S	As	Total
2272a/158		0.24			67.28		13.43	18.29	99.25
3089a/ 34	0.43	0.82		2.03	60.47	2.23	10.95	24.19	101.12

Cooperite

Cooperite occurs only occasionally as xenomorphic grains up to 100 μm across which usually contain residual Pt-Fe alloy. Concentrations of up to 6 wt.% Rh were measured with the microprobe (#3088/50). It also occurred as drop-like inclusions with traces of Pd (#3088/107) in Pt-Fe alloys.

Table 6. *Microprobe analyses of cooperite PtS*

Analysis	Ru	Rh	Pd	Os	Ir	Pt	Cu	Ni	S	Total
3088 / 50		6.00	0.81	0.32	0.88	69.12	2.75	0.93	18.39	99.22
/107			1.12	0.38		82.81			14.32	98.62
3089a/ 3				0.32		84.79	0.32		14.96	100.39

Tulameenite

One grain of this mineral was found as an individual crystal in the sample from Nawngpusawng; it was 200 μm across, euhedral, abraded at the edges, light yellow, and contained no inclusions. In addition to traces of Os and Ir, the analysis showed a Ni concentration of 2 wt.% (#2272a/152). A lathe-shaped inclusion of tulameenite was found in osmiridium (#3088/39).

Table 7. *Microprobe analyses of tulameenite Pt_2FeCu*

Analysis	Ru	Rh	Pd	Os	Ir	Pt	Fe	Cu	Ni	Total
2272a/152				0.36	0.45	75.24	9.94	9.72	2.05	97.77
3088 / 39		0.55	0.55	0.30	1.84	73.24	7.59	12.81	1.09	97.97

Isomertieite

Analysis showed a light yellow platelet about 400 μm in the sample from Manawtha to have the composition of isomertieite in which the Sb has been partially substituted by Te (#3088/3). In the same sample, as an inclusion in Pt-Fe alloys, this mineral was also found as a grain about 20 μm across grown together with sperrylite (#3088/121).

Table 8. *Microprobe analyses of isomertieite* $Pd_{11}Sb_2As_2$

Analysis	Ru	Rh	Pd	Os	Ir	Pt	Te	As	Sb	Total
3088 / 3			69.19			6.71	8.55	9.70	6.49	100.65
/121			73.38		0.31	0.33	6.62	9.79	8.96	99.40

Inclusions

Other PGM were found only as inclusions in Pt-Fe alloys, or more seldom in Os-Ir-Ru alloys and sperrylite. They were found mainly in the sample from Manawtha. Since the inclusions were usually very small (< 30 μm), a precise analysis was not always possible.

Braggite is present as a brownish pink, xenomorphic inclusion 25 μm across in a Pt-Fe alloy (#3088/155).

Table 9. *Microprobe analysis of braggite* (*Pd, Pt*)*S*

Analysis	Ru	Rh	Pd	Os	Ir	Pt	Fe	Cu	Ni	S	Te	Total
3088 /155			48.80			27.69	1.18	2.55	0.39	18.01	2.06	100.69

Platarsite and *hollingworthite* occur mainly as drop-like inclusions in Pt-Fe alloys or intergrown with each other or with gold and sperrylite. At least part of the Pt apparently detected in the hollingworthite is probably from interference by the surrounding mineral, although the corresponding Fe concentrations were extremely low. In some cases, the Ir content of the hollingworthite was as high as 18 wt.% (#3088/21). Platarsite also has a high Ir, Ru, and Rh content (15, 8, and 4 wt.%, respectively, #3088/20).

Table 10. *Microprobe analyses of platarsite PtAsS/hollingworthite RhAsS*

Analysis	Ru	Rh	Pd	Os	Ir	Pt	S	As	Total
3088 / 20	8.22	4.39		0.93	15.66	30.72	9.77	31.32	101.01
/ 21	5.17	21.65		0.85	18.68	10.25	12.88	30.24	99.72
/126	6.30	20.02		3.54	0.69	23.34	12.31	31.73	97.93

Bowieite occurs as irregular, grey-brown inclusions up to 50 μm across in Pt-Fe alloys. In contrast to the observations of *Desborough* and *Criddle* (1984), only very low concentrations of Pt and Ir were found (#3088/89 and 3089a/73). Occasionally it was observed forming composite grains with laurite.

Table 11. *Microprobe analyses of bowieite* Rh_2S_3

Analysis	Ru	Rh	Pd	Os	Ir	Pt	S	Total
3088 / 89		66.52			0.51	1.50	31.24	99.77
3089a/ 73		63.18			1.88	1.72	30.61	97.40

Keithconnite was found as a xenomorphic pink inclusion 20 μm long forming a composite grain with bowieite in the sample from Tanga (#3089a/71). The Pt content recorded in the analysis is probably from the surrounding Pt-Fe alloy.

Table 12. *Microprobe analysis of keithconnite* Pd_3Te

Analysis	Ru	Rh	Pd	Os	Ir	Pt	Te	Total
3089a/ 71			69.99			2.45	28.99	101.43

A breccia-like grain, 100 μm, of Pt-Fe alloy, iridosmine, cooperite, and a light-grey (in reflected light), isotropic mineral was found in sample #3088 (Fig. 7d). The chemical composition of the light-grey mineral (#3088/131 and 132) corresponded approximately to *cuproiridsite* (*Rudashevski* et al., 1985).

Table 13. *Microprobe analyses of cuproiridsite* $CuIr_2S_4$

Analysis	Ru	Rh	Pd	Os	Ir	Pt	Cu	S	Total
3088 /131		2.15			39.58	25.48	9.62	22.25	99.08
/132		2.33			40.45	24.60	9.95	22.50	99.83

A brownish drop-like, isotropic inclusion 20 μm across in Pt-Fe alloy (#3088/147) appears to be *malanite* on the basis of the analysis.

Table 14. *Microprobe analysis of malanite* $Cu(Pt, Ir)_2S_4$

Analysis	Ru	Rh	Pd	Os	Ir	Pt	Fe	Cu	S	Total
3088 /147		4.06			26.98	35.34	0.51	9.91	23.17	99.96

Stibiopalladinite and *geversite* occur as lobed or drop-like inclusions 25 μm long in Pt-Fe alloys with a Pt/Fe (in at.%) ratio of unity (#2272b/57, 60, 61 and 54).

Table 15. *Microprobe analyses of stibiopalladinite* Pd_5Sb_2

Analysis	Ru	Rh	Pd	Os	Ir	Pt	Cu	Ni	Sb	Total
2272b/ 57			63.13			5.84	2.90	0.42	29.87	102.15
/ 60			62.90			5.96	2.96	0.44	29.79	102.06
/ 61			62.55			5.80	3.03	0.38	29.85	101.62

Table 16. *Microprobe analysis of geversite* $PtSb_2$

Analysis	Ru	Rh	Pd	Os	Ir	Pt	As	Sb	Total
2272b/ 54				0.35		44.19	1.64	52.49	98.67

Kashinite occurs as platelet fragments of 15 μm size in cavities of Pt-Fe alloys in the sample from Indawgyi Lake (#3452/36 and 37).

Table 17. *Microprobe analyses of kashinite* Ir_2S_3

Analysis	Ru	Rh	Pd	Os	Ir	Pt	Fe	S	Total
3452 / 36		9.03			67.84	1.23	0.39	22.33	100.81
3452 / 37		6.89			71.36	2.70	0.36	21.76	103.08

Pentlandite, *pyrrhotite*, and *chalcopyrite* were also present as oriented inclusions in Pt-Fe alloys, more rarely in Os-Ir-Ru alloys. Pentlandite sometimes contained elevated Ru and Rh concentrations.

Unnamed PGM Phases

The analysis of several phases observed as inclusions in Pt-Fe and Os-Ir-Ru alloys yielded formulae that did not correspond to any previously known mineral. Almost all of these grains were smaller than 30 μm across; for this reason their optical and physical properties could not be determined. Following *Cabri* (1980), we will only give the many combinations of elements without trying to derive new minerals. Further studies would be necessary for this.

Pt-Pd-Pb-Sb probably $(Pt, Pd)_2PbSb$

Light-brown, strongly anisotropic (with brownish to bronze interference colors) platelet crystals up to 30 μm across as inclusions in Pt-Fe alloys (Pt-Fe = 1 [at.%]) (Table 18, analyses 1–4; Fig. 7e).

Table 18. *Microprobe analyses of unnamed PGM phases*

Analysis	Pd	Ir	Pt	Pb	Fe	Cu	Ni	Sb	Total
1	16.20	0.63	33.64	27.91	0.56	0.49	0.53	20.58	100.54
2	15.09	0.91	32.18	35.39			0.47	13.76	97.80
3	16.35	0.78	31.38	32.23	0.31		0.46	16.61	98.12
4	16.36	0.92	31.28	31.52			0.44	18.49	99.01

Analysis	Pd	Pt	Fe	Cu	Sb	Total
5	54.10	4.52	0.31	13.46	29.37	101.76
6	51.48	5.90	0.63	13.88	28.98	100.87

Analysis	Pd	Os	Ir	Pt	Cu	S	Total
7	71.86	0.37	0.99	0.61	12.90	12.07	98.80

Analysis	Ru	Rh	Os	Ir	Fe	Ni	S	As	Total
8	1.72	40.56	0.93	2.08	0.37	21.44	1.81	29.52	98.43

Analysis	Rh	Ir	Pt	Fe	Cu	Ni	S	Total
9	16.22	20.19	2.46	5.08	3.88	21.82	27.95	97.60

Analysis	Rh	Ir	Pt	Pb	Te	Bi	Total
10	24.20	5.67	2.72	7.09	56.05	4.98	100.71

1	$(Pt_{1.05}, Pd_{0.92}, Fe_{0.06}, Ni_{0.06}, Cu_{0.05}, Ir_{0.02})_{2.16}\, Pb_{0.82}\, Sb_{1.03}$
2	$(Pt_{1.09}, Pd_{0.94}, Ni_{0.05}, Ir_{0.03}, Fe_{0.00}, Cu_{0.00})_{2.11}\, Pb_{1.13}\, Sb_{0.75}$
3	$(Pt_{1.03}, Pd_{0.98}, Ni_{0.05}, Fe_{0.04}, Ir_{0.03}, Cu_{0.02})_{2.15}\, Pb_{0.99}\, Sb_{0.87}$
4	$(Pt_{1.02}, Pd_{0.98}, Ni_{0.05}, Ir_{0.03}, Fe_{0.00}, Cu_{0.00})_{2.08}\, Pb_{0.97}\, Sb_{0.96}$
5	$(Pd_{2.05}, Pt_{0.09})_{2.14}\, (Cu_{0.86}, Fe_{0.02})_{0.88}\, Sb_{0.97}$
6	$(Pd_{1.97}, Pt_{0.12})_{2.09}\, (Cu_{0.89}, Fe_{0.05})_{0.94}\, Sb_{0.97}$
7	$(Pd_{6.94}, Os_{0.02}, Ir_{0.05}, Pt_{0.03})_{7.04}\, Cu_{2.09}\, S_{3.87}$
8	$(Rh_{0.95}, Ru_{0.04}, Ir_{0.03}, Os_{0.01})_{1.03}\, (Ni_{0.88}, Fe_{0.02})_{0.90}\, (As_{0.95}, S_{0.14})_{1.09}$
9	$(Rh_{1.04}, Ir_{0.69}, Pt_{0.08})_{1.81}\, (Ni_{2.44}, Fe_{0.60}, Cu_{0.40})_{3.44}\, (S_{5.73}, Te_{0.01})_{5.74}$
10	$(Rh_{1.52}, Pb_{0.22}, Ir_{0.19}, Pt_{0.09})_{2.02}\, (Te_{2.83}, Bi_{0.15})_{2.98}$

Pd-Cu-Sb probably Pd_2CuSb

Brownish violet, isotropic, drop-like grains up to 15 μm across as inclusions in Pt-Fe alloys (Pt/Fe = 1 [at.%]) (Table 18, analyses 5 – 6).

Pd-Cu-S probably $Pd_7Cu_2S_4$

Isotropic, drop-like grain 10 μm across, white with a light-violet tinge, forming a composite grain with Pt-Fe alloy as inclusion in iridosmine (Table 18, analysis 7).

Rh-Ni-As probably RhNiAs

Light-brown, isotropic, cubic grain 10 μm across forming a composite grain with pentlandite as inclusion in rutheniridosmine (Table 18, analysis 8). This could

correspond to the unnamed RhNiAs from northeastern USSR described by *Rudashevski* et al. (1983).

Rh-Ni-S probably $Rh_2Ni_3S_6$

Light-gray, isotropic, cubic grain 15 μm across as inclusion in Pt-Fe alloy (Table 18, analysis 9; Fig. 7f).

Rh-Te probably Rh_2Te_3

Drop-like isotropic inclusion 15 μm long, light-gray with a light-blue tinge, in Pt-Fe alloy (Table 18, analysis 10). Though the optical properties seem to be similar to the unnamed $Rh(Te, Bi)_2$ from Ethiopia described by *Cabri* et al. (1981) the chemical analysis differs slightly.

Discussion

The petrographic study of sediment samples from the four sites in the Chindwin Basin showed a distinct decrease in grain size of the PGM from north to south. In contrast, on the basis of the microprobe analyses of the Pt-Fe and Os-Ir-Ru alloys, there is no significant change in the composition of the samples from the four sites. This indicates a common source area. The sample from Lake Indawgyi used for comparison has a mineral composition similar to those from the Chindwin Basin; however, the mean grain size was distinctly different. This sample was taken near an ophiolite complex that could be the source area. The source of the samples from the Chindwin Basin, however, is not clear and it can only be surmised that they derive from ophiolites similar to those west of Lake Indawgyi.

The textures observed, e.g. lamellar intergrowths between grains of Pt-Fe and Os-Ir-Ru alloys (Fig. 4: a and c), the numerous oriented inclusions of osmium and iridosmium lamellae in Pt-Fe alloys, and schlieren-like appearance of Pt-Fe alloys in Os-Ir-Ru alloys (Fig. 4d), unambiguously indicate that the PGM are of primary origin. This is supported by the myrmekite-like intergrowths of Os-Ir-Ru alloys with Os-Ir-Ru sulfide (Fig. 7c) and the usually euhedral PGE sulfide inclusions in the alloys. Crusts and oriented irarsite, cooperite, and laurite replacement minerals on the alloy grains are surely serpentinization products.

Conclusions

We conclude that the PGM were formed under magmatic conditions and were affected by serpentinization. The source rocks in the area around the northern Chindwin Basin were eroded and the fragments transported to the south. The data show the decrease in PGM particle size expected from fluvial transport from north to south. The reason for this decrease can be that smaller grains are carried over a longer distance than bigger ones as *Raicevic* and *Cabri* (1976) suggested for the Tulameen River Area, B.C., Canada. But this can also be the result of attrition of the particles being worn down. Unexplained, however, is how ideal crystals up to

200 μm across (Fig. 3: d and e) could survive assumed transport for several hundred kilometers.

Acknowledgments

We thank *Soe Win* for providing us with the samples from Tanga and Lake Indawgyi and for numerous discussions in the field. We also wish to thank the following members of the BGR staff: *E. Knickrehm*, for the SEM micrographs; *J. Lodziak II*, for the microprobe analyses; and *D. Laszinski*, for the computer programs to calculate structural formulae and graphic data representation. We acknowledge numerous useful discussions with Drs. *K.-P. Burgath*, *P. Müller*, and *W. Knabe*. Dr. *H. J. Unger* from the Bavarian Geological Survey provided advice on Quaternary mapping. Dr. *R. C. Newcomb* translated our manuscript. We also gratefully acknowledge the constructive criticism of two reviewers.

References

Bannert D, Helmcke D (1981) The evolution of the Asian Plate in Burma. Geol Rdsch 70: 446–458

Bender F (1983) Geology of Burma. Gebrüder Bornträger, Berlin Stuttgart, 293 pp

Cabri LJ (1980) Determination of ideal formula for new minerals of the platinum-group. XIth Int Min Assoc Meet Novosibirsk, Proc I, pp 157–165

— *Criddle AJ, Laflamme JHG, Bearne GS, Harris DC* (1981) Mineralogical study of complex Pt-Fe nuggets from Ethiopia. Bull Mineral 104: 508–525

— *Feather CE* (1975) Platinum-iron alloys: A nomenclature based on a study of natural and synthetic alloys. Can Mineral 13: 117–126

— *Harris DC* (1975) Zoning in Os-Ir alloys and the relation of the geographical and tectonic environment of the source rocks to the bulk Pt : Pt + Ir + Os for placers. Can Mineral 13: 266–274

Chattopadhyay B, Venkataramana P, Roy DK, Bhattacharyya S, Gosh S (1983) Geology of Naga Hills Ophiolites. Geol Surv India Rec 112, 2: 59–115

Desborough GA, Criddle AJ (1984) Bowieite: A new rhodium-iridium platinum sulfide in platinum-alloy nuggets, Goodnews Bay, Alaska. Can Mineral 22: 543–552

Ford RJ (1981) Platinum-Group Minerals in Tasmania. Econ Geol 76: 498–504

Goossens PJ (1978) The metallogenic provinces of Burma. 3rd Reg Conf Geol Min Res SE Asia, Bangkok, pp 495–536

Harris DC, Cabri LJ (1973) The nomenclature of the natural alloys of osmium, iridium and ruthenium based on new compositional data of alloys from world-wide occurrences. Can Mineral 12: 104–112

Raicevic D, Cabri LJ (1976) Mineralogy and concentration of Au- and Pt-bearing placers from the Tulameen River Area in British Columbia. CIM Bull 770: 111–119

Reiman KU, Aye Thaung (1981) Palynostratigraphic investigation of the Tertiary Chindwin basin. 4th Int Palyn Conf, Lucknow, India (1976–1977), pp 380–395

Rudashevski NS, Menshikov YR, Mochalov AG, Trubkin NV, Shumskaya NI, Zhdanov VV (1985) Cuprorhodsite $CuRh_2S_4$ and cuproiridsite $CuIr_2S_4$—new natural thiospinels of platinum group elements. Zapiski Vses Mineral Obshch 119: 187–195 (in Russian)

— *Mochalov AG, Menshikov YP, Shumskaya NI* (1983) Ferronickel-platinum, Pt_2FeNi, a new mineral species. Zapiski Vses Mineral Obshch 112: 487–494 (in Russian)

Stumpfl EF, Tarkian M (1973) Natural osmium-iridium alloys and iron-bearing platinum: new electron probe and optical data. N Jb Miner Mh 7/8: 312–322

Tarkian M (1987) Compositional variations and reflectance of the common platinum-group minerals. Mineral Petrol 36: 169–190

Authors' addresses: Dr. *D. Hagen* and Dr. *Th. Weiser*, Bundesanstalt für Geowissenschaften und Rohstoffe, Stilleweg 2, D-3000 Hannover 51, Federal Republic of Germany, *Than Htay*, Department of Geological Survey and Exploration, Kanbe Rd., Yankin P.O., Rangoon, Burma.

Correspondence should be addressed to Dr. *Th. Weiser*.